ELSEVIER

Chemical Physics 270 (2001) 165–175

Chemical Physics

www.elsevier.com/locate/chemphys

Third-order transport properties of ions in electrostatic fields

Andreas D. Koutselos

Physical Chemistry Laboratory, Department of Chemistry, National and Kapodistrian University of Athens, Panepistimiopolis, 15771 Athens, Greece

Received 27 December 2000; in final form 2 May 2001

Abstract

Third-order transport properties are calculated through a three-temperature kinetic theory for ions moving in gases under the action of a homogeneous electrostatic field. The analytic procedure is found to be in good agreement with independently obtained numerical results, as well as with calculations from molecular dynamics simulation of the ionic motion. Finally, a relation which enables the calculation of all components of third-order transport coefficients from characteristic integrals of velocity correlation functions is suggested and tested successfully. © 2001 Elsevier Science B.V. All rights reserved.

1. Introduction

The transport of a swarm of non-reactive ions in neutral gases under the influence of a homogeneous electrostatic field has been investigated thoroughly in the past [1], primarily through the study of mobility and ion-diffusion coefficients [2]. Occasionally velocity distribution (**v**-distribution) moments and angular momentum alignment relative to the field have also been studied experimentally [3–5]. Higher-order transport properties have not been measured so far, though they have been suspected to influence experimental results [6]. The interpretation of traditional drift tube experiments, however, does not require the consideration of such properties [1].

Relevant transport coefficients are defined through expansion of the ion flux in terms of density gradients [7] as follows

$$\mathbf{J} = n\mathbf{v_d} - \mathbf{D}\nabla n + \mathbf{Q} : \nabla\nabla n + \cdots, \tag{1}$$

where n is the ion density, $\mathbf{v_d}$ is the mean (drift) velocity, **D**, **Q**, etc. are transport coefficients of second, third etc. order (and rank). The gradients multiply externally and the contraction of their rank through scalar product with the transport coefficients leads to a vector. For simplicity dots are used to designate only multiple contraction. The Fickian diffusion coefficient, **D**, due to the symmetry of the ion motion as imposed by the electric field, acquires two independent components, D_{ZZ} and $D_{XX} = D_{YY}$, with the field in the z-direction. Similarly, with the additional requirement of irrelevance to the order of differentiation in Eq. (1), **Q** has seven non-vanishing components, three of which are independent, Q_{ZZZ}, $Q_{ZXX} = Q_{ZYY}$ and $Q_{XZX} = Q_{XXZ} = Q_{YZY} = Q_{YYZ}$.

Until now only the Q_{ZZZ} component has been determined through solution of the Boltzmann kinetic equation for Li^+ in He and Ar [8], and two components of the symmetric form of **Q**, Q_{ZZZ} and $\overline{Q} = (Q_{ZXX} + Q_{XXZ} + Q_{XZX})/3$, for K^+ in Ar have been obtained from a non-equilibrium molecular dynamics (MD) simulation of the ion motion [9–11].

Contrary to this, the experimental determination of 'Burnett-level' **Q** coefficients has to await

0301-0104/01/$ - see front matter
PII: S0301-0104(01)00395-0

the development of experimental techniques which are sensitive to high-order transport. The knowledge of **Q** in advance, however, can help in the design and interpretation of future experiments. For this purpose, in the following we extend the three-temperature moment method for the solution of the Boltzmann kinetic equation that describes the ionic motion in an electrostatic field, so that all components of the third-order transport coefficients become accessible. This approach has been proven to be efficient in providing transport properties and comparable in accuracy to more elaborate methods at low and high field strengths developed in the past [12]. In addition, the method is used for the testing and analysis of the two **Q** components calculated in the past by MD simulations. Though an interpretation of the form of the $\overline{Q}$ component has been presented in the past [9], triggered by the analysis of Vrhovac et al. [13] of the form of third-order **Q** tensor, testing was missing due to lack of knowledge of relevant **Q** components. The present method will allow the calculation of all three components of **Q** through the moment solution of Boltzmann kinetic equation and will permit the testing of the MD results. In addition, a conjecture will be introduced that will allow the calculation of all three **Q** components from characteristic velocity correlation (**v**-correlation) integrals obtainable from simulation methods [9,11].

In the following, the method is first tested through comparison of calculated low-order transport properties, such as mobility, ion-diffusion coefficients and moments of the distribution function, against independently determined accurate numerical results for an inverse power potential model and a representative alkali ion–noble gas system. Further, third-order transport properties are compared against results of the kinetic theory and a non-equilibrium MD simulation of the ion motion.

2. Theory

The system consists of a small amount of ions moving in a low-density gas under the action of an electrostatic field. The ions move independently of each other but acquire non-equilibrium **v**-distributions through the action of the external field and collisions with the gas molecules. The gas itself is not disturbed from equilibrium since it is present in excess. Such conditions are utilized experimentally in drift tube mass spectrometers [1].

Under the above conditions only the number density can vary (weakly) in space and the ion flux can be analyzed according to Eq. (1). In addition, all time derivatives except $\partial n/\partial t$ must vanish. With these considerations the Boltzmann kinetic equation for the **v**-distribution function of the ions, $f(\mathbf{v})$, can be transformed in a moment equation [7],

$$\frac{\partial}{\partial t}(n\langle\psi\rangle) + \nabla(n\langle\mathbf{v}\psi\rangle) - (q\mathbf{E}/m)n\langle\nabla_{\mathbf{v}}\psi\rangle = -n\langle J\psi\rangle, \tag{2}$$

where q and m are the charge and the mass of the ions, respectively, n is the ion-number density, **E** is the electric field, ψ is an arbitrary function of the velocity **v** and the brackets refer to averaging over $f(\mathbf{v})$,

$$n\langle\psi\rangle = \int f(\mathbf{v})\psi(\mathbf{v})\mathrm{d}\mathbf{v}. \tag{3}$$

Finally, J is the usual ion–atom Boltzmann collision operator with Gaussian **v**-distribution for the gas.

To eliminate the time dependent term from the above equation we employ the continuity equation which can be obtained from the same equation on setting $\psi \equiv 1$,

$$\frac{\partial n}{\partial t} = -\nabla(n\langle\mathbf{v}\rangle). \tag{4}$$

Finally, by substituting $\partial n/\partial t$ from the above equation in Eq. (2), we obtain

$$n\langle J\psi\rangle = (q\mathbf{E}/m)n\langle\nabla_{\mathbf{v}}\psi\rangle - \nabla(n\langle\mathbf{v}\psi\rangle) + \langle\psi\rangle\nabla(n\langle\mathbf{v}\rangle). \tag{5}$$

Before proceeding to the final stage of determining moment equations for **Q** we expand the ion **v**-distribution in terms of a set of orthogonal basis functions, $\psi_{pqr}(\mathbf{v})$, as follows

$$f(\mathbf{v}) = f^0(\mathbf{v})\sum_{pqr}\alpha_{pqr}\psi_{pqr}(\mathbf{v}), \tag{6}$$

where α_{pqr} are expansion coefficients and $f^0(\mathbf{v})$ is a zero-order approximation to the distribution function. According to the three-temperature theory [15] this function acquires the form of a displaced elliptic Gaussian,

$$f^0(\mathbf{v}) = Z\exp(-w_x^2 - w_y^2 - w_z^2), \tag{7}$$

where Z is normalization factor and

$$w_x^2 = mv_x^2/2kT_\perp, \quad w_y^2 = mv_y^2/2kT_\perp, \tag{8}$$

$$w_z^2 = m(v_z - v_\mathrm{d})^2/2kT_\parallel. \tag{9}$$

Here, v_x, v_y and v_z are cartesian ion-velocity components and the electirc field is assumed to be in the z-direction. The corresponding basis functions are defined through

$$\psi_{pqr}(\mathbf{v}) = H_p(w_x)H_q(w_y)H_r(w_z), \tag{10}$$

where H_n is Hermite polynomial of order n. The ψ_{pqr} are orthogonal and have as weight functions the zero-order $\mathbf{v}$-distribution $f^0(\mathbf{v})$.

We can now simplify the collision term of the moment equations by inserting the expansion of the $\mathbf{v}$-distribution in the collision operator and obtain

$$\langle J\psi\rangle = N\sum_{stu} b(pqr;stu)\langle\psi_{stu}\rangle, \tag{11}$$

with

$$b(pqr;stu) = \int f^0(\mathbf{v})\psi_{stu}(\mathbf{v})J\psi_{pqr}(\mathbf{v})\mathrm{d}\mathbf{v} \Big/ \int f^0(\mathbf{v})\psi_{stu}(\mathbf{v})^2\mathrm{d}\mathbf{v}. \tag{12}$$

The parameters v_d, $T_\perp$ and $T_\parallel$ can be chosen in various ways. Here we define them through the first few moments of the $\mathbf{v}$-distribution of a homogeneous reference system,

$$v_\mathrm{d} = \langle v_z\rangle^0, \tag{13}$$

$$\tfrac{1}{2}kT_\perp = \tfrac{1}{2}m\langle v_x^2\rangle^0 = \tfrac{1}{2}m\langle v_y^2\rangle^0, \tag{14}$$

$$\tfrac{1}{2}kT_\parallel = \tfrac{1}{2}m\langle(v_z - v_\mathrm{d})^2\rangle^0, \tag{15}$$

where $\langle\,\rangle^0$ denotes averaging over $f(\mathbf{v})$ of the reference system, i.e. over $f^0(\mathbf{v})$. This choice of parameters leads to constrains upon the expansion coefficients, namely

$$\alpha_{001} = \alpha_{010} = \alpha_{100} = \alpha_{002} = \alpha_{020} = \alpha_{200} = 0. \tag{16}$$

Transport properties can be obtained from the above moment equations through expansion of $\mathbf{v}$-moments in terms of density gradients as follows,

$$n\langle\psi_{pqr}\rangle = n\langle\psi_{pqr}\rangle^0 - \sum_i \langle\psi_{pqr}\rangle_D^i \frac{\partial n}{\partial r_i} + \sum_{i,j}\langle\psi_{pqr}\rangle_Q^{ij}\frac{\partial^2 n}{\partial r_i\partial r_j}, \tag{17}$$

where r_i represents cartesian spatial coordinates, x, y and z. First, relations between transport coefficients and $\mathbf{v}$-moments are obtained by setting $\psi_{100} = (2m/kT_\perp)^{1/2}v_x$, or $\psi_{001} = (2m/kT_\parallel)^{1/2}\times(v_z - v_\mathrm{d})$ in the above equation and comparing the resulting expression with Eq. (1). The terms of first order in the gradient give

$$D_{ZZ} = \frac{1}{2\beta_\parallel}\langle\psi_{001}\rangle_D^Z, \tag{18}$$

$$D_{XX} = \frac{1}{2\beta_\perp}\langle\psi_{100}\rangle_D^X, \quad D_{YY} = \frac{1}{2\beta_\perp}\langle\psi_{010}\rangle_D^Y, \tag{19}$$

where $\beta_{\parallel,\perp} = (m/2kT_{\parallel,\perp})^{1/2}$. Hereafter we set $D_\parallel \equiv D_{ZZ}$ and $D_\perp \equiv D_{XX} = D_{YY}$. The next order in density gradient produces third-order transport coefficients the three independent components of which are denoted by $Q_\parallel \equiv Q_{ZZZ}$, $Q_X \equiv Q_{ZXX}$ and $Q_\perp \equiv Q_{XZX} = Q_{XXZ}$. These definitions hold also with Y in the place of X. The resulting relations are

$$Q_\parallel = \frac{1}{2\beta_\parallel}\langle\psi_{001}\rangle_Q^{ZZ}, \tag{20}$$

$$Q_X = \frac{1}{2\beta_\parallel}\langle\psi_{001}\rangle_Q^{XX}, \tag{21}$$

$$Q_\perp = \frac{1}{4\beta_\perp}\left(\langle\psi_{100}\rangle_Q^{XZ} + \langle\psi_{100}\rangle_Q^{ZX}\right). \tag{22}$$

Further, the expansion for the moments, Eq. (17), is substituted into the moment Eq. (5), taking into account the expression for the ion flux, Eq. (1),

$$\nabla(n\langle\mathbf{v}\rangle) = \nabla\mathbf{J} = \mathbf{v}_\mathrm{d}\nabla n - \mathbf{D}:\nabla\nabla n + \mathbf{Q}\vdots\nabla\nabla\nabla n + \cdots \tag{23}$$

The whole expression can then be separated into three sets of equations; one equation relating the homogeneous moments, $\langle\psi\rangle^0$, alone, a second equation relating the first-order expanded moments with the homogeneous ones and, finally, a third equation relating the second-order expanded moments with the lower order ones. The first and second equations are identical to the ones derived in the past [14,15] and need not be repeated here, the third set, however, is new and leads to the calculation of third-order transport coefficients. It is

$$\sum_{stu} b(pqr;stu)\langle\psi_{stu}\rangle_Q^{ij} = 2r\varepsilon\langle\psi_{pq(r-1)}\rangle_Q^{ij} + h_{pqr}^{ij}, \tag{24}$$

where

$$h_{pqr}^{ZZ} = (1/2N\beta_\parallel)\left[\langle\psi_{pq(r+1)}\rangle_D^Z + 2r\langle\psi_{pq(r-1)}\rangle_D^Z\right] - D_{ZZ}\langle\psi_{pqr}\rangle^0, \tag{25}$$

$$h_{pqr}^{XX} = (1/2N\beta_\perp)\left[\langle\psi_{(p+1)qr}\rangle_D^X + 2p\langle\psi_{(p-1)qr}\rangle_D^X\right] - D_{XX}\langle\psi_{pqr}\rangle^0, \tag{26}$$

$$h_{pqr}^{XZ} = (1/2N\beta_\perp)\left[\langle\psi_{(p+1)qr}\rangle_D^Z + 2p\langle\psi_{(p-1)qr}\rangle_D^Z\right], \tag{27}$$

$$h_{pqr}^{ZX} = (1/2N\beta_\parallel)\left[\langle\psi_{pq(r+1)}\rangle_D^X + 2r\langle\psi_{pq(r-1)}\rangle_D^X\right], \tag{28}$$

and $\varepsilon = qE\beta_\parallel/mN$. The last two equations as written are unsymmetrized, in the sense that they refer to $\langle\psi_{stu}\rangle_Q^{ij}$ moments that are not invariant upon interchange of i and j. Though one can combine h_{pqr}^{XZ} with h_{pqr}^{ZX} and obtain a new equation for symmetric moments, we prefer to keep the equations separate, here, for simplicity. The final $Q_\perp$ components will then be given by Eq. (22), though the moments $\langle\psi_{100}\rangle_Q^{XZ}$ and $\langle\psi_{100}\rangle_Q^{ZX}$ will not emerge equal to one another from Eq. (24).

The above moment equations must be solved under the following restrictions,

$$\langle\psi_{000}\rangle_Q^{ij} = 0;\ \langle\psi_{pqr}\rangle_Q^{ZZ} = \langle\psi_{qpr}\rangle_Q^{ZZ}, \tag{29}$$

$$\begin{aligned}&\langle\psi_{pqr}\rangle_Q^{XZ,ZX} = 0 \text{ for all odd } q;\\ &\langle\psi_{qpr}\rangle_Q^{ZZ,XX} = 0 \text{ for all odd } p \text{ or } q.\end{aligned} \tag{30}$$

We mention that all the **Q** components can be obtained from the above moment equations and therefore there is no need to consider terms with Y coordinates in the position of X ones. We also see that the above obtained equations for second-order density-perturbed moments are compatible to the ones derived by Larsen et al. [8], though the latter have been derived through expansion of the distribution function and the present through expansion of the **v**-distribution moments.

All of the sets of moment equations, the ones obtained here and the ones derived in the past [15], are coupled. Therefore, in order to obtain a solution, one must start by solving the lower order sets of equations and then proceed to higher order ones. In this way, we begin by solving the equations for the homogeneous moments [15], $\langle\psi_{pqr}\rangle^0$, starting from an initial guess for v_d, $T_\perp$ and $T_\parallel$ parameters. Subsequently, we determine the above parameters from the implicit dependence of $b(001;000)$, $b(200;000)$ and $b(002;000)$ on them and repeat the previous step until convergence at the fifth significant figure is attained. The values of all three parameters are then fixed and the mobility is obtained from $K = v_\mathrm{d}/E$. Further, we proceed to the solution of equations for the first-order density-perturbed moments, $\langle\psi_{pqr}\rangle_D^i$, from which diffusion coefficients are calculated through Eqs. (18) and (19). Finally, with the use of the previously determined moment equations, ((24)–(28)), second-order density-perturbed moments, $\langle\psi_{pqr}\rangle_Q^{ij}$, are calculated and from them third-order diffusion coefficients are obtained through Eqs. (20)–(22).

In order to apply the procedure to ion-atom systems the moment series has to be truncated. Here, we employ the truncation scheme of Lin et al. [15], according to which, at an order of approximation n, terms with $(s+t+u) \geqslant (n+2)$ are eliminated from the homogeneous moment equations. For first-order perturbed moments the first requirement becomes $(s+t+u) \geqslant (n+1)$ and for second-order moments we require

$(s+t+u) \geqslant n$. Finally, the same hold for the sum $(p+q+r)$.

We proceed now to the testing of the present procedure against accurate calculations of transport properties for a model potential and certain ion–atom systems.

3. Applications for low-order ion properties

Having obtained moment equations for second-order density-perturbed moments we can determine all the components of the third-order transport coefficient through the procedure outlined above. However, before proceeding to the calculation of **Q**, we first test the accuracy of our procedure against independent, accurate kinetic theory calculations for low-order transport properties of an inverse power model potential as well as of a representative alkali ion–noble gas system, K^+ in Ar.

3.1. R^{-8} model potential

The resulting drift velocities, effective temperatures and diffusion coefficients parallel and perpendicular to the field calculated from our computer program should approach very close to, if not coincide with, the three-temperature theory calculations of the past. This is, because the two methods differ only in details, mainly in the implementation of the solution of the moment equations and the calculation of the matrix elements of the Boltzmann collision term. In the present calculations the cross sections and the collision integrals have been obtained through the numerical method of Barker et al. [16], extended to accommodate two temperature Gaussian **v**-distribution functions. In addition, the quadrature points in the Gauss–Legendre integration have been quadrupled and the range of integration doubled. Such improvements slow down the calculations but increase the accuracy of the cross-sections beyond the fourth significant figure, as has been inferred from testing against accurate results of various n-6-4 model potentials [17].

The whole method has been tested against accurate results for various inverse-power model potentials. As a typical example we present drift velocities, effective temperatures and diffusion coefficients in Table 1 for an R^{-8} model potential in the cold-gas limit, $T = 0$, together with results calculated by Skullerud [18] using the Wannier moment method. In the same table, we present third-order transport properties for future comparisons. We thus observe that within the fifth approximation reasonable convergence occurs mainly at high ion–neutral mass ratios.

The two sets of results for the low-order transport properties differ by about 1%, except in the case of diffusion coefficients and at small ion–neutral mass ratio, where differences up to a few percent are observed. This behavior is characteristic of the three-temperature theory, as has been observed in the past by Lin et al. [15].

To confirm this coincidence we proceed to the testing of the transport properties of a representative alkali ion–noble gas system.

3.2. K^+ in Ar

The low-order ion-transport properties by now can be determined quite accurately through various kinetic theory methods [8,12,15,19] at any ion–neutral mass ratio and over a wide field range. Here, we compare our results for K^+ in Ar using the universal interaction model potential [20] to transport properties obtained through the Gram–Charlier (GC) treatment of the Boltzmann equation [19] and accessed through Viehland's data base as described in Ref. [21]. The accuracy attained by this method for the mobility is better than 1%, and the effective ion temperatures and various moments of the **v**-distribution function [19] are calculated within a few percent. These properties together with the present results are reported in Table 2.

We find that the differences between ion properties calculated using our fifth approximation and the results of the GC method are at the level of accuracy of the latter approach, except at intermediate and occasionally at very high field strengths where the three-temperature theory does not fully converge. This is a known behavior of the theory and is caused from the inflexibility of the expansion of the distribution function to

Table 1
Transport properties obtained in the fourth and fifth approximation of the three-temperature theory as a function of mass ratio for R^{-8} potential in the cold-gas limit and with $v_d = 1000$ m/s, together with accurate reference data calculated by Skullerud [18]

m/M		$v_d/(\alpha\lambda)^{2/3}$	$kT_\parallel/Mv_d^2$	$kT_\perp/Mv_d^2$	$\alpha D_\parallel/\frac{M}{m}v_d^3$	$\alpha D_\perp/\frac{M}{m}v_d^3$	$10\alpha^2 Q_\parallel/(\frac{M}{m})^2 v_d^5$	$10\alpha^2 Q_X/(\frac{M}{m})^2 v_d^5$	$10\alpha^2 Q_\perp/(\frac{M}{m})^2 v_d^5$
0.10	4	0.6732	0.3559	0.3220	0.2305	0.3236			0.649
	5	0.6723	0.3566	0.3228	0.2328	0.3260			0.668
	SK	0.67	0.36	0.32	0.23	0.32			
0.20	4	0.7904	0.3658	0.3096	0.2319	0.3044			0.645
	5	0.7898	0.3662	0.3099	0.2352	0.3077			0.693
	SK	0.790	0.367	0.309	0.23	0.30			
0.50	4	1.046	0.3712	0.2826	0.2357	0.2724			
	5	1.044	0.3718	0.2833	0.2297	0.2769			
	SK	1.047	0.369	0.282	0.222	0.270			
1.0	4	1.384	0.3652	0.2590	0.2358	0.2516			
	5	1.384	0.3634	0.2593	0.2207	0.2518			
	SK	1.387	0.361	0.258	0.220	0.248			
2.0	4	1.930	0.3615	0.2407	0.2326	0.2364	1.382	0.189	0.768
	5	1.931	0.3590	0.2403	0.2234	0.2353	1.539	0.229	0.867
	SK	1.932	0.360	0.240	0.227	0.233			
3.0	4	2.393	0.3628	0.2334	0.2335	0.2301	1.516	0.249	0.825
	5	2.394	0.3614	0.2330	0.2300	0.2293	1.512	0.263	0.880
	SK	2.395	0.361	0.234	0.231	0.230			
4.0	4	2.811	0.3647	0.2295	0.2358	0.2269	1.572	0.282	0.858
	5	2.811	0.3641	0.2293	0.2346	0.2264	1.526	0.286	0.888
	SK	2.813	0.363	0.231	0.235	0.228			
$\gg 1$	4	21.634	0.3768	0.2176	0.2509	0.2174	1.736	0.382	0.941
	5	21.634	0.3768	0.2176	0.2509	0.2174	1.735	0.382	0.941
	SK	21.544	0.3774	0.2169	0.2516	0.2169			

The quantity m/M is the ion–atom mass ratio, $\alpha = qE/m$ is the acceleration of the ion and $\lambda = 1/N\Gamma_1$, with $\Gamma_1 = 1.0770\pi(2/\mu)^{1/4}$, and μ the relative mass.

reproduce the form of the actual **v**-distribution as it is distorted, presumably due to partial or actual runaway of the ions. The consequences of this effect are more pronounced in the case of the ion-diffusion coefficients at intermediate field strengths, where only low-order calculations produce reasonable results [12].

Diffusion coefficients parallel and perpendicular to the field are compared in Fig. 1 with the results from the GC procedure, which are known with an accuracy of 1%. Again, the differences of the two sets of data are around 1%, except at intermediate fields where the present calculations have not converged and at strong fields where they reach a value of 2%. This behavior is general and has also been observed for various alkali ion–noble gas systems which have been tested using universal interaction model potentials [20].

4. Applications for third-order ion properties

The above comparisons test successfully the present implementation of the three-temperature moment solution of Boltzmann kinetic equation. We proceed to examine the calculation of **Q** components of two ion–atom systems for which third-order transport properties have been determined independently, from kinetic theory and non-equilibrium MD simulation methods.

Table 2
Transport properties obtained in the fourth and fifth approximation of the three-temperature theory for K^+ in Ar at 300 K, together with accurate results obtained through the GC treatment of the Boltzmann equation [19] (the moments are defined in Ref. [21])

E/N (Td)		Ko (cm^2/Vs)	$T_\parallel$ (K)	$T_\perp$ (K)	$1+$SKEW	KURz	KURx	$1+$C1	C2	$ND_\parallel$ (10^{20}/ms)	$ND_\perp$ (10^{20}/ms)
1.000	4	2.621	300.1	300.1	1.001	3.000	3.000	1.000	1.000	1.821	1.821
	5	2.621	300.1	300.1	1.001	3.000	3.000	1.000	1.000	1.821	1.821
	GC	2.624	300.1	300.1	1.001	3.000	3.000	1.000	1.000	1.823	1.823
10.56	4	2.625	312.0	307.4	1.016	3.004	3.004	1.005	1.001	1.904	1.869
	5	2.625	312.0	307.4	1.016	3.004	3.004	1.005	1.001	1.904	1.869
	GC	2.629	313.1	306.9	1.017	3.004	3.004	1.005	1.001	1.912	1.867
20.19	4	2.640	344.9	327.9	1.070	3.040	3.028	1.021	1.011	2.147	2.005
	5	2.640	345.0	327.9	1.070	3.041	3.028	1.021	1.011	2.149	2.005
	GC	2.644	348.5	325.6	1.071	3.041	3.026	1.021	1.010	2.171	1.992
42.07	4	2.741	524.6	439.2	1.372	3.434	3.307	1.128	1.127	3.880	2.810
	5	2.736	524.4	439.0	1.378	3.478	3.320	1.128	1.135	3.887	2.818
	GC	2.743	534.0	425.3	1.369	3.440	3.282	1.121	1.119	3.904	2.723
61.19	4	2.895	872.8	643.3	1.743	4.139	3.865	1.277	1.345		
	5	2.874	850.5	643.8	1.720	4.281	3.876	1.265	1.366		
	GC	2.898	880.7	607.7	1.710	4.070	3.798	1.262	1.321	7.827	4.252
80.09	4	3.015	1351	928.1	1.921	4.494	4.223	1.362	1.462		
	5	3.049	1333	931.4	1.818	4.380	4.177	1.334	1.435		
	GC	3.043	1377	882.8	1.855	4.338	4.160	1.341	1.380	12.10	6.427
102.04	4	3.160	2060	1371	1.891	4.236	4.273	1.372	1.421		
	5	3.217	2110	1394	1.813	4.014	4.263	1.355	1.382		
	GC	3.174	2097	1308	1.867	4.160	4.255	1.361	1.423	16.27	9.712
207.12	4	3.147	6323	4199	1.668	3.452	3.950	1.283	1.206		29.76
	5	3.143	6339	4182	1.684	3.425	3.963	1.290	1.201		29.74
	GC	3.152	6356	4109	1.673	3.434	3.946	1.278	1.210	32.38	30.33
306.73	4	2.877	10762	7330	1.620	3.557	3.838	1.256	1.171	48.62	47.33
	5	2.873	10739	7312	1.642	3.346	3.836	1.261	1.168	48.49	47.46
	GC	2.883	10725	7271	1.625	3.477	3.853	1.252	1.184	49.14	46.93
404.08	4	2.662	15523	10732	1.606	3.337	3.802	1.246	1.164	64.22	64.12
	5	2.659	15464	10718	1.630	3.332	3.792	1.251	1.161	62.15	64.38
	GC	2.667	15526	10669	1.608	3.371	3.838	1.245	1.157	60.59	63.14
500.06	4	2.498	20636	14400	1.602	3.336	3.791	1.243	1.163	80.34	80.77
	5	2.496	20542	14393	1.627	3.334	3.777	1.247	1.161	76.62	81.17
	GC	2.503	20645	13346	1.604	3.364	3.826	1.241	1.163	75.86	80.29
617.69	4	2.344	27463	19309	1.603	3.342	3.791	1.242	1.166	101.3	101.6
	5	2.342	27323	19311	1.628	3.343	3.773	1.246	1.163	95.71	102.2
	GC	2.348	27459	19262	1.604	3.375	3.827	1.240	1.160	94.63	100.6
818.63	4	2.154	40523	28718	1.608	3.361	3.804	1.243	1.174	140.7	139.1
	5	2.152	40301	28737	1.633	3.366	3.784	1.247	1.171	131.8	140.0
	GC	2.158	40511	28687	1.609	3.393	3.841	1.242	1.167	131.1	138.0
1009.96	4	2.027	54703	38867	1.618	3.408	3.827	1.247	1.184	184.0	177.3
	5	2.025	54497	38942	1.667	3.480	3.807	1.252	1.189	170.9	178.8
	GC	2.031	54556	38862	1.617	3.412	3.857	1.245	1.191	172.4	177.8

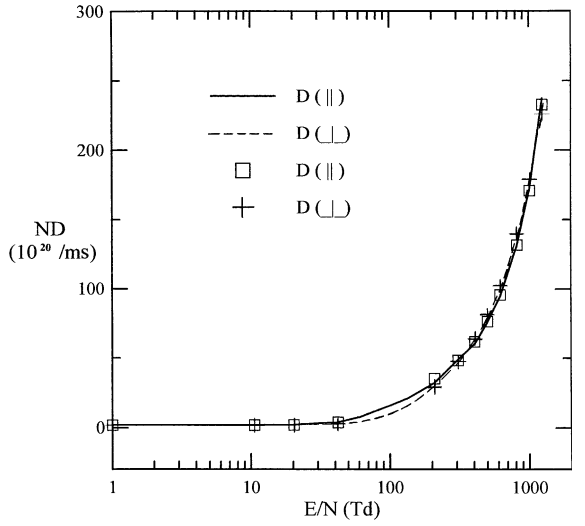

Fig. 1. Diffusion coefficients parallel and perpendicular to the field for K^+ in Ar at 300 K as function of E/N (1 Td $\equiv 10^{-21}$ Vm^2). The lines represent GC calculations [19] and the symbols present results.

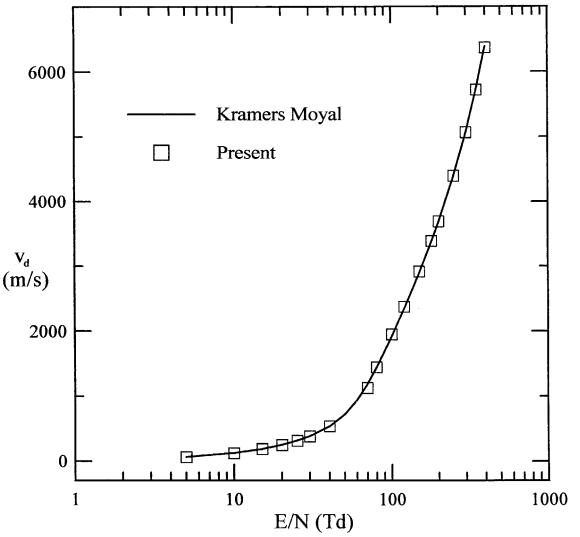

Fig. 2. Drift velocity for Li^+ in Ar at 295 K as function of E/N. The lines represent KM calculations [8], and the squares present results.

4.1. Li^+ in Ar

Accurate mobility, ion-diffusion coefficients and the Q_{ZZZ} component for Li^+ in Ar have been obtained by Larsen et al. [8] through a Kramers–Moyal (KM) expansion of Boltzmann collision integral. The low order of these transport properties have been compared by Ness and Viehland [12] to results of two- and three-temperature theory as well as against bimodal distribution function methods using the same ion–atom mobility-modified interaction potential [8]. They have all been found to be in agreement over a wide field range except at intermediate fields, where convergence of the many-temperature methods cannot be attained easily, if at all. We mention that subsequently a GC moment method has been developed by Viehland [19], with minor convergence difficulties.

The present results are obtained with implementation of the mobility-modified numerical potential of Larsen et al. [8] in our method through the interpolation scheme of Barker et al. [16]. Tests with increased data points have shown that this interpolation scheme introduces errors below 1%. The drift velocities differ from the results of the KM [8] method by about 1–2%, except at intermediate fields where deviations up to 5% are observed, as shown in Fig. 2. A similar comparison for the ion-diffusion coefficients parallel and perpendicular to the field is presented in Fig. 3 with differences within a few percent. Such differences are in conformity to deviations observed in the past from similar comparisons between three-temperature results and KM calculations [12].

In the case of Q_{ZZZ}, we present predictions in Fig. 4 together with the KM results. The observed differences are within 10%, which are comparable to the joint uncertainty of both data sets.

In the same figure (Fig. 4), we present predicted $Q_\perp$ components, $(Q_\perp = Q_{XZX} = Q_{XXZ})$, for future comparisons. We observe that within 10% accuracy the order of magnitude of $Q_\perp$ is comparable to that of Q_{ZZZ}. Therefore, this component together with Q_{ZZZ} merit attention in future attempts of experimental determination. The Q_X (Q_{ZXX}) component, however, is one order of magnitude smaller than the other components, so it does not appear to be significant in the ion transport of this system. Here, Q_X converges well only at weak fields.

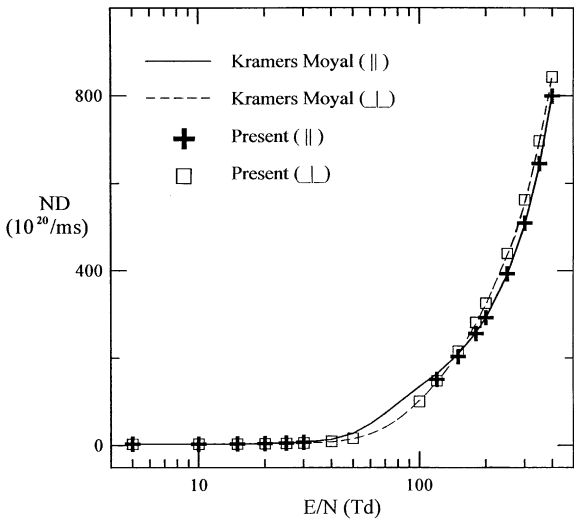

Fig. 3. Diffusion coefficients parallel and perpendicular to the field for Li^+ in Ar at 295 K as function of E/N. The lines represent KM calculations [8], and the symbols present results.

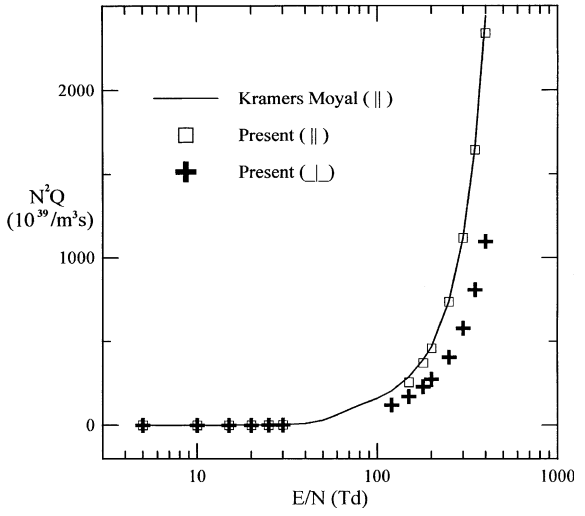

Fig. 4. Components of third-order transport coefficients, $Q_{\parallel}$ and $Q_{\perp}$, for Li^+ in Ar at 295 K as function of E/N. The lines represent KM calculations [8], and the symbols present results.

The above successful testing establishes independently the accuracy of all **Q** components and allows us to proceed next to comparison of the **Q** components against MD simulation results and confirm their form and accuracy.

4.2. K^+ in Ar

Components of the **Q** transport coefficient of K^+ in Ar have been calculated through a non-equilibrium MD simulation of the ion motion in the neutral gas [9–11]. The resulting components, denoted here $Q_{\parallel}$ and $\overline{Q}$, as have been interpreted to belong to the symmetric form of **Q**, relate to cartesian components through

$$\begin{aligned} Q_{\parallel} &= Q_{ZZZ} \\ \overline{Q} &= (Q_{ZXX} + Q_{XXZ} + Q_{XZX})/3. \end{aligned} \tag{31}$$

Their attained accuracy, which is 7–10% at intermediate fields with increasing uncertainty at weak and strong fields, is enough as to allow us to draw conclusions about their legitimacy and further seek for a better interpretation of the simulation results.

Though comparisons between the simulation results for low-order transport properties and kinetic theory calculations have been presented in the literature [10,11], we repeat them here for better assessment of the conformity of the two methods. Thus, using the same universal interaction model potential [20] we find that the mobility and ion-diffusion coefficients differ by 1% and 2–5%, respectively, over the field range, except at intermediate field strengths where the latter coefficients do not converge. Such differences are typical between MD simulation and three-temperature theories and have been observed in the past [10,11].

Similar comparisons for $Q_{\parallel}$ and $\overline{Q}$, presented in Fig. 5, show differences up to 10% over a wide field region where convergence occurs, except at very weak fields where third-order coefficients tend to zero and comparison between vanishing quantities produce large percentage errors. Since the convergence of the kinetic theory results and simulation errors are better than, or of the same magnitude to, the observed deviations we conclude that the two approaches are in agreement to each other.

Further, since $\overline{Q}$ was calculated through the MD simulation from $\overline{Q} = (B + C + D)/3$, where B, C and D are characteristic **v**-correlation integrals defined elsewhere [11], and in the present theory through Eq. (31), it is tempting to seek for

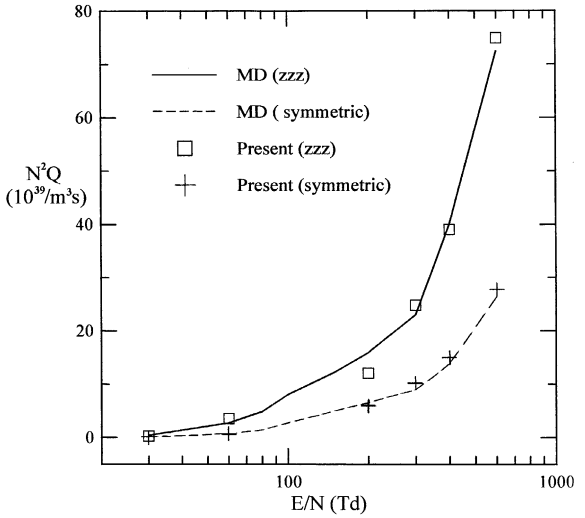

Fig. 5. Components of third-order transport coefficients, $Q_{\parallel}$ and $\overline{Q} \equiv (Q_{ZXX} + Q_{XXZ} + Q_{XZX})/3$, for K^+ in Ar at 300 K as function of E/N. The lines represent MD simulation calculations [11], and the symbols present results.

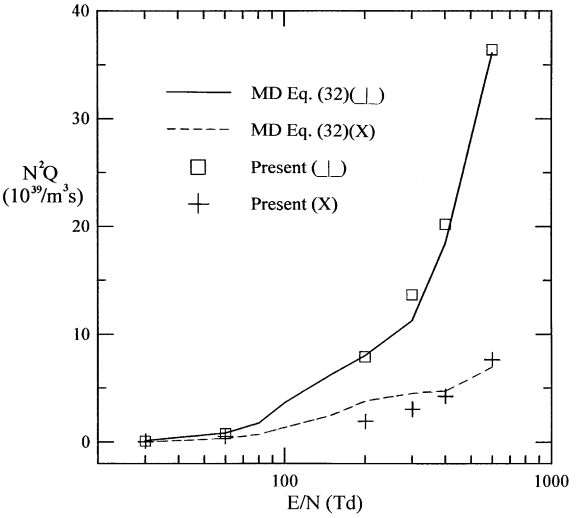

Fig. 6. Same as Fig. 5, for $Q_{\perp}$ and Q_X components. The lines represent calculations through Eq. (32), with **v**-correlation integrals from MD simulations [11], and the symbols present results.

a possible relation between actual **Q** components and **v**-correlation integrals. By examining the magnitudes of the cartesian components calculated through the three-temperature theory and the characteristic **v**-correlation integrals of the MD simulation method [11], as well as the symmetry of exchange of the two last indexes of Q_{ijk}, we infer that one can set

$$\begin{aligned} Q_{\perp} &= (B + D)/2 \\ Q_X &= C, \end{aligned} \tag{32}$$

where $C \cong D$ within the accuracy of the method. Comparisons of **Q** components calculated from these relations against three-temperature theory results are presented in Fig. 6. The observed deviations are below the uncertainty of both sets of data indicating that probably all the **Q** components can be extracted from the characteristic **v**-correlation integrals [11]. However, since the above relations remain ambiguous at the level of accuracy of the present results, they have to be considered as conjectures awaiting further testing. In addition, since the **Q** components were obtained from a hypothetical expansion of the **v**-distribution function which has not been tested completely for its ability to produce high-order transport properties the whole method for the calculation of **Q** of appropriate symmetry, Eqs. (24)–(28), has to be tested eventually through experiment.

5. Conclusions

The three-temperature kinetic theory for the transport of ions has been extended to the calculation of third-order transport coefficients. Testing of the obtained Q_{ZZZ} component for Li^+ in Ar against independently calculated accurate analytic results established the accuracy of the present procedure. Further comparisons against MD simulation results of Q_{ZZZ} and $\overline{Q}$ components for K^+ in Ar indicated that the two procedures are in agreement with each other. Finally, a conjecture about the possibility of obtaining all three independent **Q** components from MD simulations using third-order **v**-correlation functions has been suggested. Each **Q** component has been associated with a characteristic time integral of **v**-correlation functions which can be obtained through simulation of the ion motion. This conjecture should be

tested for more ion–atom systems, and the overall calculation of third-order transport coefficients should be confirmed experimentally in the future.

Acknowledgements

The author would like to thank the Institute of Computer Science of the National University of Athens for the computer time provided in their CONVEX computer. This work was supported by grants from the Research Fund of the National University of Athens, no. 70/4/3336.

References

[1] E.A. Mason, E.W. McDaniel, Transport Properties of Ions in Gases, Wiley, New York, 1988.
[2] L.A. Viehland, E.A. Mason, At. Data Nucl. Data Tables 60 (1995) 77, and earlier publications in this data compilation series.
[3] R.A. Dressler, J.P.M. Beijers, H. Meyer, S.M. Penn, V.M. Bierbaum, S.R. Leone, J. Chem. Phys. 89 (1988) 4707.
[4] M.J. Bastian, C.P. Lauenstein, V.M. Bierbaum, S.R. Leone, J. Chem. Phys. 98 (1993) 9496.
[5] R.A. Dressler, H. Meyer, S.R. Leone, J. Chem. Phys. 87 (1987) 6029.
[6] J.H. Schummers, G.M. Thomson, D.R. James, I.R. Gatland, E.W. McDaniel, Phys. Rev. A 7 (1973) 683.
[7] J.H. Whealton, E.A. Mason, Ann. Phys. NY 84 (1974) 8.
[8] P.-H. Larsen, H.R. Skullerud, T.H. Lovaas, Th. Stefansson, J. Phys. B 21 (1988) 2519.
[9] A.D. Koutselos, J. Chem. Phys. 110 (1999) 3256 (The first term on the RHS of Eq. (2) has been misprinted, it should have been $-\mathbf{v_d}\mathbf{V}n$).
[10] A.D. Koutselos, J. Chem. Phys. 104 (1996) 8442.
[11] A.D. Koutselos, J. Chem. Phys. 106 (1997) 7117.
[12] K.F. Ness, L.A. Viehland, Chem. Phys. 148 (1990) 255.
[13] S.B. Vrhovac, Z.L. Petrovic, L.A. Viehland, T.S. Santhanam, J. Chem. Phys. 110 (1999) 2423.
[14] L.A. Viehland, E.A. Mason, Ann. Phys. NY 91 (1974) 499.
[15] S.L. Lin, L.A. Viehland, E.A. Mason, Chem. Phys. 37 (1979) 411.
[16] J.A. Barker, W. Fock, F. Smith, Phys. Fluids 7 (1964) 897.
[17] L.A. Viehland, E.A. Mason, W.F. Morrison, M.R. Flannery, At. Data Nucl. Data Tables 16 (1975) 495.
[18] H.R. Skullerud, J. Phys. B 9 (1976) 535.
[19] L.A. Viehland, Chem. Phys. 179 (1994) 71.
[20] A.D. Koutselos, E.A. Mason, L.A. Viehland, J. Chem. Phys. 93 (1990) 7125.
[21] L.A. Viehland, C.C. Kirkpatrick, Int. J. Mass Spectrom. Ion Processes 149/150 (1995) 555.